Article ID: 1003－6326(2003)04－0849－06

Numerical modelling of microstructure forming process for Al-Al_3Fe eutectic alloy①

LI Rong-de(李荣德), ZHOU Zhen-ping(周振平)
(School of Materials Science and Engineering, Shenyang University of Technology, Shenyang 110023, China)

Abstract: A self-adjusting model was presented on the basis of the effect of temperature gradient on eutectic growth and a curved solid/liquid interface. Finite differential method was adopted to solve the model. The average lamellar spacing of the Al-Al_3Fe eutectic alloy and the content fields ahead of the solidifying interface under different growth rates were calculated. Directional solidification experiments were carried out in order to prove the modification of the modeling. The experimental results are in relatively good agreement with the calculations.

Key words: Al-Fe eutectic alloy; numerical modelling; growth rate; lamellar spacing
CLC number: TG 249.4 **Document code:** A

1 INTRODUCTION

Eutectic spacing is an important parameter which reflects the feature of eutectic microstructure. Study on eutectic solidification theory places mainly on the selection mechanism of eutectic spacing and morphology transition. In 1966 Jackson and Hunt[1] initially established a comparatively perfect growth theoretical models(J-H model) for normal eutectic alloy and presented selection mechanism for lamellar and rod eutectic spacing and transition condition for microstructural morphology. Subsequently researchers made a further perfection and correction on this model, making it apply to wider circumstances. These theoretical models make it possible for people to simulate eutectic growth processes.

Up to now, the numerical simulations of alloy microstructures have been made great progress[2-5]. As for eutectic alloys, the numerical simulations include two sides: one is the microstructural morphology simulation[6] and the other is the eutectic spacing[7]. The normal eutectic simulation has been great successful. However, abnormal eutectic simulation is still not desirable. Although there are much research results, theoretically abnormal eutectic models still need to be further improved. Studies on the relationship between eutectic spacing and temperature gradient are rare. Lamellar spacing is only related to growth rate R, not to temperature gradient G in the classical eutectic growth theory. For normal eutectic the effect of temperature gradient is little and can be ignored in most cases. However, the effect of temperature gradient on abnormal eutectic is obvious. Experiments show that average lamellar spacing $\bar{\lambda}$ has a fixed relationship with temperature gradient G for a given alloy. Eutectic growth model can be described by[8]

$$\bar{\lambda}^2 R = Af(G) \quad (1)$$

where A is a coefficient related to alloy compositions.

Theoretical calculation indicates that J-H model applies only to normal eutectic alloy. Magnin and Kurz et al[7] made a modification to this model. For abnormal eutectic alloy, an operating point factor, φ, was introduced. The effect of temperature gradient on undercooling should be considered due to a curved solid/liquid interface. However, all these models are based on stable solute diffusion equation and can't reflect the changing process of lamellar spacing with time. Furthermore, analytical methods are employed to solve the diffusion equation. Boundary conditions are also simplified in order to get a simple solution, regarding the interface composition as eutectic concentration, which has an obvious deviation from case especially when the growth rate is high. Moreover, density differences among eutectic phases are not taken into account. To settle the defects of models above, a solute transfer equation related to time is developed in this article and numerical method is used to simulate the relationship between average lamellar spacing and temperature gradient when growth is in stable state. There is no necessity to simplify boundary conditions because of adopting a numerical method. So it agrees better with fact. At the same

① **Received date:** 2002－06－03; **Accepted date:** 2002－10－08
Correspondence: LI Rong-de, Professor, PhD; Tel: +86-24-25691688; E-mail: lrd@sut.edu.cn

time density factor is introduced to correct the density difference among eutectic phases.

2 EXPERIMENTAL

Eutectic Al-2% Fe (mass fraction) alloy was prepared from pure aluminum and iron. Melting was carried out in a graphite crucible by using a resistance-heated furnace. Alloy was cast and oxidized film was subsequently removed. Specimens with d10 mm × 100 mm were solidified in corundum tube in a directional solidification furnace under different temperature gradient and variable growth rates. The temperature gradient in the experiment was 9.8 K/mm.

The lamellar spacings were measured on metallographs[9] of longitudinal section of the specimen, about 10 mm behind the quenched interface to ensure being in the steady state region. The average spacing was obtained from measurement (over 100 lamellar spacings) in various representative areas of the specimen. These measurements were carried out perpendicular to the general direction of the lamellae in very carefully selected regions where the lamellar is more or less kept constant over some areas within the grains. But these regions are not limited to those where the lamellae are strictly parallel since the latter are not representative of the overall microstructure. The measurements are listed in Table 2. Fitting the relationship between average experimental lamellar spacing $\bar{\lambda}$ and growth rate R an experiential formula is obtained:

$$\bar{\lambda}^{2.26}R = 1\,479\ \mu m^{3.26}/s \quad (2)$$

3 ESTABLISHMENT OF MATH MODEL

3.1 Content field controlling equation and corresponding boundary conditions

Fig. 1 shows a growing schematic diagram at a given growth rate for lamellar α(Al) and Al_3Fe phase in eutectic Al-Al_3Fe alloy. λ is the average simulative lamellar spacing. Considering the periodicity of eutectic microstructure and the symmetry of content field in a spacing, $\lambda/2$ is a calculated object. Rectangular coordinate is established whose origin is three-phase junction, growth direction is along y axis.

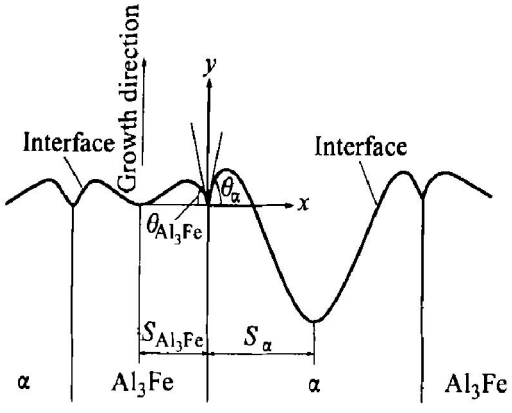

Fig. 1 Simplified lamellar interface morphology for Al-Al_3Fe eutectic alloy

Hypotheses are made in order to simplify calculation before setting up mathematical model:

1) In the course of calculating content field, suppose that interface be curved, that is to say, the effect of interface curvature on content field is neglected. But when calculating the undercooling, solid/liquid interface is regarded as curved surface. Not only the effect of curvature, but also the effect of temperature gradient on undercooling should be taken into account.

Such hypotheses are reasonable. The exact solution to content field can not be obtained because the real interface shape is unknown. However, under general growth rate Peclet($p = \lambda R/2D$) is very small and the amplitude of interface is much less than diffusion distance. Therefore, real interface shape can't affect the solution to diffusion equation.

Although the exact interface shape is not known, it should satisfy at least following requirements:

To α(Al):

$$(dy/dx)|_{x=0} = \tan\theta_\alpha$$

$$(dy/dx)|_{x=S_\alpha} = 0$$

$$y|_{x=S_\alpha} = -\delta_\alpha$$

$$y|_{x=0} = 0$$

To Al_3Fe phase:

$$(dy/dx)|_{x=0} = -\tan\theta_{Al_3Fe}$$

$$(dy/dx)|_{x=-S_{Al_3Fe}} = 0$$

$$y|_{x=S_{Al_3Fe}} = -\delta_{Al_3Fe}$$

$$y|_{x=0} = 0$$

Four conditions can determine four unknowns. So the interface equation can be assumed as $y = ax^3 + bx^2 + cx + d$ and undetermined coefficients can be used to determine a, b, c and d. y is

$$y = \begin{cases} S_\alpha\tan\theta_\alpha[(2\varphi+1)(\lambda x/S_\alpha)^3 - (3\varphi+2)(\lambda x/S_\alpha)^2 + (\lambda x/S_\alpha)] & (\alpha\ \text{phase}) \\ S_{Al_3Fe}\tan\theta_{Al_3Fe}[(2\varphi+1)(-\lambda x/S_{Al_3Fe})^3 - (3\varphi+2)(-\lambda x/S_{Al_3Fe})^2 + (-\lambda x/S_{Al_3Fe})] & (Al_3Fe\ \text{phase}) \end{cases} \quad (3)$$

2) Liquid volume is limitless. The change of liquid content in the infinite distance ahead of interface is neglected during calculation.

3) The diffusion of solute in solid is ignored.

Ordering $w = w(x, y)$ to be the solute content at any point of liquid in front of interface, the content field controlling equation is

$$\frac{\partial w}{\partial t} = D\left[\frac{\partial^2 w}{\partial x^2} + \frac{\partial^2 w}{\partial y^2}\right] + R\frac{\partial w}{\partial y} \tag{4}$$

The variation range of independent variable in this model is $-S_{Al_3Fe} \leqslant x \leqslant S_\alpha$ and $0 \leqslant y < +\infty$. Lamellar spacing $\lambda = \lambda(t)$ varies with time. Introducing dimensionless rectangular coordinates X and Y, ordering $X = x/\lambda$, $Y = y/\lambda$ and substituting them into above-mentioned equation gives

$$H\frac{\partial w}{\partial t} = \frac{\partial^2 w}{\partial X^2} + \frac{\partial^2 w}{\partial Y^2} + N\frac{\partial w}{\partial Y} \tag{5}$$

Obviously, the variation range of X and Y is $-f_{Al_3Fe}/2 \leqslant X \leqslant f_\alpha/2$ and $0 \leqslant Y < +\infty$, respectively.

Corresponding boundary conditions are

1) Periodicity

To arbitrary X having

$$w(X+1) = w(X) \tag{6}$$

2) Symmetry

$$\frac{\partial w}{\partial X} = 0 \quad (X = -f_{Al_3Fe}/2,\ X = f_\alpha/2) \tag{7}$$

3) Far field condition

$$w(\vec{Y} + \infty) = w_E \tag{8}$$

4) Local equilibrium condition

neglecting solute diffusion in solid, the conservation of solute at the interface requires

$$-D\frac{\partial w}{\partial Y}\Big|_{Y=0} = R(w_{int} - w_S) \tag{9}$$

Considering the relationship of content in liquid with that in solid, the densities of eutectic phases are different, so the expression above can be written by

$$\left.\frac{\partial w}{\partial Y}\right|_{Y=0} = \begin{cases} -\dfrac{v_\alpha R}{D} w_{\alpha,int}(1-k_\alpha) & (\alpha \text{ phase}) \\ \dfrac{v_{Al_3Fe}R}{D}(1-w_{Al_3Fe,int})(1-k_{Al_3Fe}) & (Al_3Fe \text{ phase}) \end{cases} \tag{10}$$

Note that $w_{\alpha,int}$ and $w_{Al_3Fe,int}$ are the real content at interface, not the eutectic content w_E regarded by Jackson or Magnin et al.

3.2 Undercooling calculation

After calculating the content field ahead of interface, the undercooling ΔT_i of each eutectic phase can be derived:

$$\Delta T_i = \Delta T_{i,c} + \Delta T_{i,r} + \Delta T_{i,k} \tag{11}$$

1) Solute content $\Delta T_{i,c}$

$$\Delta T_{i,c} = m_i(w_E - w_{i,int}) \tag{12}$$

2) Curvature undercooling $\Delta T_{i,r}$

$$\Delta T_{i,r} = \Gamma_i K(X) = -\Gamma_i \frac{\dfrac{d^2Y}{dX^2}}{\left[1+\left(\dfrac{dY}{dX}\right)^2\right]^{3/2}} \tag{13}$$

3) Kinetic undercooling $\Delta T_{i,k}$

To normal eutectic the kinetic undercooling can be ignored. To abnormal eutectic, one of the eutectic phases is faceted phase which has a larger kinetic undercooling. But kinetic undercooling does not have obvious effect on eutectic growth in general conditions. Therefore it can be still ignored[10].

4) Effect of temperature gradient G on undercooling

If temperature gradient G exists at interface it certainly leads to the change of undercooling. For simplification, suppose that G be constant and its direction be perpendicular to interface. Because of the small depth of interface depression, the undercooling variation $\Delta T_{i,G}$ resulting from G can be approximately expressed by

$$\Delta T_{i,G} = GY(X) \tag{14}$$

After deriving $\Delta T_{i,c}$, $\Delta T_{i,r}$, $\Delta T_{i,G}$ the average undercooling $\overline{\Delta T_i}$ of phase i can be calculated:

$$\overline{\Delta T_i} = \overline{\Delta T_{i,c}} + \overline{\Delta T_{i,r}} + \overline{\Delta T_{i,G}} \tag{15}$$

where $\overline{\Delta T_{i,c}} = m_i \dfrac{1}{f_i}\displaystyle\int_0^{f_i}(w_E - w_{i,int})\,dX$,

$\overline{\Delta T_{i,r}} = \Gamma_i \overline{K}(X) = 2\Gamma_i \sin\theta_i/(\lambda f_i)$,

$\overline{\Delta T_{i,G}} = G\overline{Y}(X) = G(-\delta_i/2 + \lambda f_i \tan\theta_i/24)$

Note that δ_i is unknown and should be tried to solve. Constraining the undercooling in the center of phase i equal to average undercooling of phase i gives the δ_i expressions:

$$\delta_\alpha = [-m_\alpha(w_E - w_{\alpha,int})(X = f_\alpha/2) - 4\Gamma_\alpha \tan\theta_\alpha/(\lambda f_\alpha) - \overline{\Delta T_{\alpha,c}} - \overline{\Delta T_{\alpha,r}} - G\lambda f_\alpha \tan\theta_\alpha/24]/[2/G + 24\Gamma_\alpha/(\lambda f_\alpha)^2] \tag{16}$$

$$\delta_{Al_3Fe} = [-m_{Al_3Fe}(w_E - w_{Al_3Fe,int})(X = f_{Al_3Fe}/2) - 4\Gamma_{Al_3Fe}\tan\theta_{Al_3Fe}/(\lambda f_{Al_3Fe}) - \overline{\Delta T_{Al_3Fe,c}} - \overline{\Delta T_{Al_3Fe,r}} - G\lambda f_{Al_3Fe}\tan\theta_{Al_3Fe}/24]/[2/G + (\lambda f_{Al_2Fe})^2] \tag{17}$$

Having δ_i expression $\overline{\Delta T_\alpha}$ and $\overline{\Delta T_{Al_3Fe}}$ can be given.

So average undercooling $\overline{\Delta T}$[10] of eutectic phases are obtained:

$$\overline{\Delta T} = \frac{|m_\alpha|\,\overline{\Delta T_{Al_3Fe}} + m_{Al_3Fe}\overline{\Delta T_\alpha}}{|m_\alpha| + m_{Al_3Fe}} \tag{18}$$

3.3 Lamellar spacing selection

Undercooling ΔT and lamellar spacing λ require

$$\Delta T = K_1 R\lambda + K_2/\lambda \tag{19}$$

The spacing is determined by undercooling. For normal eutectic alloy in steady growth, the spacing should make the undercooling minimum at a given growth rate. But for abnormal eutectic, steady spacing departures from extremum theorem. Therefore, the spacing must be corrected, introducing operating point factor φ. Experiments show that the value of φ is independent of growth rate under general growth rate. Abnormal eutectic average spacing λ[11] is

$$\lambda = \varphi\lambda_{ex} \tag{20}$$

Differentiating Eqn. (19) and ordering $d\Delta T/d\lambda = 0$ as well as combining Eqn. (20) finally get spacing selection formula

$$\lambda\Delta T = (\varphi^2 + 1)K_2 \quad (21)$$

Eqn. (21) only shows the spacing selection law in steady growth state. For unstable growth, the spacing and undercooling are uncertain to satisfy the relationship above. It is assumed in the paper that undercooling and spacing still satisfy Eqn. (21). With the help of the assumption the solidification microstructure parameters in stable growth state are worked out. In a given solidification condition of λ and R, using Eqns. (3)~(10) the content field ahead of interface is calculated; using Eqns. (11)~(18) the undercooling is calculated and finally using Eqn. (21) spacing at this moment is worked out. Serving the calculated results as the initial conditions of the next time, the spacing and undercooling are calculated. The process is self-adjustment of λ with time. The calculation is over when the relative error of undercooling (or spacing) between the last and next time is less than the given precision (for example, 10^{-5}).

4 SIMULATION RESULTS AND ANALYSES

4.1 Comparison of calculated spacings with experimental results of Al-2%Fe eutectic alloy

The relationship between λ and R in eutectic Al-2%Fe alloy is calculated and the calculations are also compared with experimental results. The physical properties of Al-2% Fe eutectic alloy are listed in Table 1. The results of calculations are listed in Table 2.

It is shown in Table 2 that not only the experimental spacings but the calculation results all decrease with the increase in growth rate. The departures are relatively large when the growth rate is low, but small error occurs at high growth rate. The large departures at low growth rates are related mainly to the simplified interface in the paper. The real solid/liquid interface of abnormal eutectics is more complex than that assumed by the paper. It can be concluded that the assumed interface is more different from the real interface at low growth rate and little different at high growth rate. The agreement between the results is acceptable. The relationship of calculation with experimental spacings satisfies

$$\lambda^2 R = 881\ \mu m^3/s \quad (22)$$

Table 1 Physical parameters of Al-2%Fe eutectic alloy

Symbol	Value	Reference
w_E	2.0	[12]
m_α	-2.8	[13]
m_{Al_3Fe}	41.7	[13]
$w_{0,\alpha}$	0.052	[12]
w_{0,Al_3Fe}	52.1	[12]
ρ_α	2.5	4/
ρ_{Al_3Fe}	3.7	[14]
f_α	0.94	4/
f_{Al_3Fe}	0.06	4/
Γ_α	0.11	[12]
Γ_{Al_3Fe}	0.16	[12]
θ_α	65	[12]
θ_{Al_3Fe}	30	[12]
D	925.5	[12]
φ	5.0	[12]

Table 2 Comparison of experimental lamellar spacings of Al-%2Fe eutectic alloy with calculated ones under different growth rates at temperature gradient of 9.8 K/mm

Growth rate/($\mu m \cdot s^{-1}$)	Spacing/μm	
	Experimental	Calculated
3.41	15.24	15.95
4.33	12.40	14.19
9.03	9.49	9.86
25.00	6.00	5.93
31.67	5.79	5.27
40.28	5.06	4.68
66.45	3.79	3.64

4.2 Distribution of content ahead of solidifying interface

Fig. 2 shows the calculated distribution of content ahead of solid/liquid interface. The growth

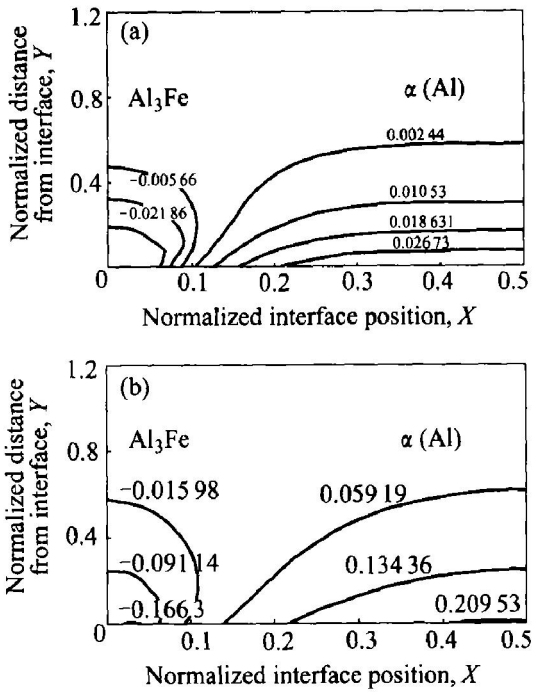

Fig. 2 Content field ahead of solidifying interface of Al-2%Fe eutectic
(a) —R = 10 $\mu m/s$; (b) —R = 100 $\mu m/s$

rates are 10 μm/s and 100 μm/s, respectively. Fig. 2 only gives the content isolines in a half width of lamellar spacing due to the symmetry of content. It shows that the degree of solute affluence(α(Al)) or scarcity(Al_3Fe) is slight when the growth rate is low, but that is heavy when the growth rate is high. Besides, the degree in the center of phases is the heaviest. With the increase in distance from phase center the solute content gradually declines. In the growth direction, with the increase in distance from interface the solute content also decreases. Solute affluence or scarcity only exists in short range (about a lamellar spacing). The solute in liquid is still well-distributed beyond the distance.

4.3 Effect of temperature gradient *G* on lamellar spacing

Table 3 lists the calculated spacing values at different growth rates when G is 0 K/mm. Compared with Table 2, it reveals that the effect of G variation on lamellar spacing is small. So the effect of temperature gradient can be ignored. However, the effect of G is remarkable when the growth rate is very low($R < 0.1$ μm/s). It can be found in Fig. 3 that temperature gradient, G, has a notable effect on lamellar spacing, λ. It indicates that the non-isothermal phenomenon of interface is serious and the effect of temperature gradient on eutectic growth must be taken into account.

At the same time, the calculation reveals that the operating point factor φ is no longer a constant

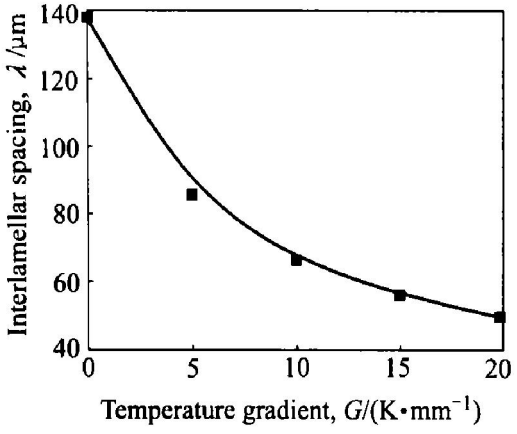

Fig. 3 Effect of temperature gradient on lamellar spacing($R = 0.05$ μm/s)

Table 3 Calculation of inter-lamellar spacings under different growth rates($G = 0$ K/mm)

Growth rate, R/(μm·s^{-1})	Calculated spacing, λ/μm
3.41	16.07
4.33	14.26
9.33	9.87
25.00	5.93

but the function of growth rate R. As shown in Fig. 4, φ declines with the decrease in growth rate under the same temperature gradient. At this moment the relationship of $\lambda^2 R =$ constant is no longer tenable.

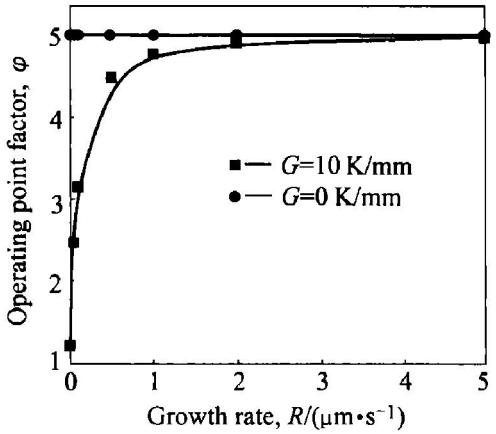

Fig. 4 Effect of growth rate on operating point factor

5 CONCLUSIONS

Based on the effect of temperature gradient on eutectic growth and a curved interface, a self-adjusting model with time is established. The calculated and experimental lamellar spacings of Al-2% Fe eutectic alloy are compared. Following results can be drawn:

1) Average lamellar spacing decreases with the increase in growth rate. Furthermore, both the experimental and calculated results are in good agreement. The relationships between lamellar spacing and R are

$\lambda^{2.26} R = 1\,479$ μm$^{3.26}$/s

$\lambda^2 R = 881$ μm^3/s, respectively

2) The calculated content field shows that content isolines is symmetrically distributed with parabola shape on the whole. The farther the distance from interface, the slighter the solute affluence or scarcity is; and the higher the growth rate is, the more serious the solute affluence or scarcity is. Solute uniformity in liquid only exists in a very short range. Beyond this range solute distribution is also uniform.

3) When the growth rate is higher the effect of temperature gradient on lamellar spacing is smaller, which can be ignored. But when the growth rate is very low interface is no longer isothermal. Here temperature gradient has a remarkable effect on spacing and must be considered. In the meantime, the operating point factor φ is no more a constant, but varies with growth rate. So the relationship of $\lambda^2 R =$ constant is untenable.

i —α(Al) or Al_3Fe phase

R —Growth rate, μm/s

λ—Average simulative lamellar spacing, μm

$\overline{S_i}$ —Half width of phase i, μm

$\overline{\lambda}$ —Average experimental lamellar spacing, μm

f_i —Volume fraction of phase i, $f_i = 2S_i\sqrt{\lambda}$

λ_{ex} —Extremum lamellar spacing, μm

ρ_i —Density of phase i, g/cm^3

$\overline{\rho}$ —Average density, $\overline{\rho} = f_\alpha\rho_\alpha + f_{Al_3Fe}\rho_{Al_3Fe}$, g/cm^3

v_i —Density factor of phase i, $v_i = \rho_i/\overline{\rho}$

w_E —Eutectic content (mass fraction), %

$w_{i,int}$ —Solute content of liquidus phase i at interface (mass fraction), %

$\overline{w}_{i,int}$ —Average content in liquidus phase i at interface (mass fraction), %

w_s —Solute content of solid phase (mass fraction), %

T_E —Eutectic temperature, K

$H = \lambda^2/D$

$N = \lambda R/D$

m_i —Liquidus slope of phase i, K/%

$\overline{M}$ —Average liquidus slope of phase i, $\overline{M} = \dfrac{|m_\alpha| m_{Al_3Fe}}{|m_\alpha| + m_{Al_3Fe}}$, K/%

G —Thermal gradient, K/mm

φ —Operating point factor, $\varphi = 2\delta_i/(\lambda_i\tan\theta_i)$

D —Diffusivity coefficient of iron in liquid aluminum, μm^2/s

k_i —Distribution coefficient of phase i

Γ_i —Gibbs-Thompson coefficient of phase i, μm·K

θ_i —Contact angle of phase i at three-phase junction, (°)

$\kappa(x)$ —Curvature at any point of interface

$\overline{\kappa}(X)$ —Average curvature of phase i at interface

ΔT_i —Growth undercooling of phase i, K

$\Delta\overline{T}_i$ —Average growth undercooling of phase i, K

$\Delta T_{i,c}$ —Solute undercooling of phase i, K

$\Delta\overline{T}_{i,c}$ —Average solute undercooling of phase i, K

$\Delta T_{i,r}$ —Curvature undercooling of phase i, K

$\Delta\overline{T}_{i,r}$ —Average curvature undercooling of phase i, K

$\Delta T_{i,k}$ —Kinetic undercooling, K

$\Delta T_{i,G}$ —Undercooling from thermal gradient, K

$\Delta\overline{T}_{i,G}$ —Average undercooling from thermal gradient, K

$\Delta\overline{T}$ —Average undercooling of eutectic phases, K

δ_i —Depression depth in center of phase i, μm

$K_1 = (\overline{M}C_{i,0}/D)(P/f_{f\,Al_3Fe})$, K·s/μm^2

$w_{i,0} = v_\alpha(w_E - w_{0,\alpha}) + v_{Al_3Fe}(w_{0,Al_3Fe} - w_E)$, %

$w_{0,i}$ —Solid solubility of phase i in the other phase (mass fraction), %

$$P = \sum_{n=1}^{\infty}\frac{1}{(n\pi)^3}\sin^2(n\pi f_\alpha) = \sum_{n=1}^{\infty}\frac{1}{(n\pi)^3}\sin^2(n\pi f_{Al_3Fe})$$

$$K_2 = -2\overline{M}\left(\frac{\Gamma_\alpha\sin\theta_\alpha}{|m_\alpha| f_\alpha} + \frac{\Gamma_{Al_3Fe}\sin\theta_{Al_3Fe}}{m_{Al_3Fe} f_{Al_3Fe}}\right)$$

x, y —Rectangular coordinates, μm

a, b, c, d —Arbitrary constants

X, Y —Dimensionless rectangular coordinates

REFERENCES

[1] Jackson K A, Hunt J D. Lamellar and rod eutectic growth [J]. Trans AIME, 1966, 236(8): 1129-1142.

[2] Steinbach I, Beckemanmm C. Three-dimensional modeling of equiaxed dendritic growth on a mesoscopic scale [J]. Acta Mater, 1999, 47(3): 971-982.

[3] Boettinger W J, Warren J A. Simulation of the cell to plane front transition during directional solidification at high velocity [J]. J Cryst Growth, 1999, 200: 583-591.

[4] Lu J W, Cheng F J. Assessment of mathematical models for the flow in directional instability [J]. Phys Rev E, 2001, 63: 1-4.

[5] Du Q, Li D Z. Simulation a double casting technique using level set method [J]. Comp Mater Sci, 2001, 22: 200-212.

[6] Stefanescu D M, Kanetkar C S. Modeling microstructural evolution of eutectic cast iron and of the gray/white transition [J]. AFS Trans, 1987, 95: 139-144.

[7] Magnin P, Kurz W. An analytical model of irregular eutectic growth and its application to Fe-C [J]. Acta Metall, 1987, 35(5): 1119-1128.

[8] Kassner K, Misbah C. Similarity laws in eutectic growth [J]. Physical Review Letters, 1991, 66(4): 27-33.

[9] Li R D, Li S J, Yu H P, et al. Growth process of Al_3Fe phase in Al-2.0% Fe eutectic alloy under unidirectional solidification [J]. Chinese Journal of Mechanical Engineering, 2000, 36(6): 82-86. (in Chinese)

[10] Nagnin P, Mason J T, Rivedi R T. Growth of irregular eutectics and the Al-Si system [J]. Acta Metall Mater, 1991, 39(4): 469-480.

[11] Grugel R N, Lograssor T A, Hellawell A. The solidification of monotectic alloys microstructures and phase spacing [J]. Metall Mater Trans A, 1984, 15A: 1003-1011.

[12] Gilgien P, Zryd A, Kurz W. Microstructure selection maps for Al-Fe alloys [J]. Acta Metall Mater, 1995, 43(9): 3477-3487.

[13] Mcleod A J, Hogan L M, Adam C M, et al. Growth mode of the aluminium phase in Al-Si and Al-Al_3Fe eutectics [J]. J Crystal Growth, 1973, 19: 301-309.

[14] Mondolfo L F, WANG Zhu-tang, ZHANG Zhen-lu, et al. Structures and Properties of Aluninum Alloys [M]. Beijing: Metallurgical Industry Press, 1984. (in Chinese)

(Edited by YANG Bing)